

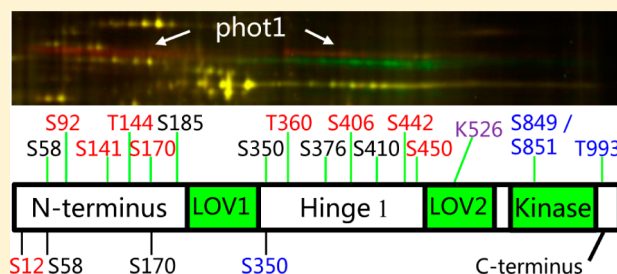
Blue Light-Induced Proteomic Changes in Etiolated *Arabidopsis* Seedlings

Zhiping Deng,^{†,‡,⊥} Juan A. Oses-Prieto,^{§,⊥} Ulrich Kutschera,[†] Tong-Seung Tseng,[†] Lingzhao Hao,^{‡,||} Alma L. Burlingame,[§] Zhi-Yong Wang,^{*,†} and Winslow R. Briggs[†][†]Department of Plant Biology, Carnegie Institution for Science, Stanford, California 94305, United States[‡]State Key Laboratory Breeding Base for Zhejiang Sustainable Pest and Disease Control, Institute of Virology and Biotechnology, Zhejiang Academy of Agricultural Sciences, Hangzhou 310021, China[§]Department of Pharmaceutical Chemistry, University of California–San Francisco, San Francisco, California 94158, United States^{||}College of Life Science, Hebei Normal University, Shijiazhuang 050024, China

Supporting Information

ABSTRACT: Plants adapt to environmental light conditions by photoreceptor-mediated physiological responses, but the mechanism by which photoreceptors perceive and transduce the signals is still unresolved. Here, we used 2D difference gel electrophoresis (2D DIGE) and mass spectrometry to characterize early molecular events induced by short blue light exposures in etiolated *Arabidopsis* seedlings. We observed the phosphorylation of phototropin 1 (phot1) and accumulation of weak chloroplast movement under blue light 1 (WEB1) in the membrane fraction after blue light irradiation. Over 50 spots could be observed for the two rows of phot1 spots in the 2-DE gels, and eight novel phosphorylated Ser/Thr sites were identified in the N-terminus and Hinge 1 regions of phot1 in vivo. Blue light caused ubiquitination of phot1, and K526 of phot1 was identified as a putative ubiquitination site. Our study indicates that post-translational modification of phot1 is more complex than previously reported.

KEYWORDS: *Arabidopsis*, blue light, phototropins, protein phosphorylation, signal transduction



INTRODUCTION

Because they are sessile, plants have evolved to respond adaptively to their ever-changing light environment by photoreceptor-mediated physiological responses. Plants possess several families of photoreceptors that can sense light direction, duration, quality, and quantity, including red and far-red photoreceptors (phytochromes) and three classes of UV-A/blue photoreceptors (cryptochromes, phototropins, and members of the Zeitlupe family).^{1,2} These photoreceptors use light signals to regulate almost every phase of plant growth and development, from seed germination through flowering and senescence. For example, phototropins mediate a number of blue light responses in *Arabidopsis thaliana*, including phototropism, chloroplast movement, leaf flattening, leaf positioning, stomatal opening, and rapid inhibition of growth of dark-grown seedlings,^{1,3–5} thus optimizing light capture for plant photosynthesis and growth.

Fifteen years ago, Christie et al.⁶ first demonstrated that phototropin 1 (phot1) acts as a blue light/UV-A receptor for phototropism in land plants. This membrane-associated photoreceptor was the first of a family of two (phot1 and phot2), and a great deal has been learned about its structure and photochemistry.^{3,7} Its two flavin-binding domains (designated LOV1 and LOV2) have been extensively studied by

flash photolysis, FTIR, resonance Raman spectroscopy, and absorption and fluorescence spectroscopy, among other biophysical techniques.⁷ With the discovery that LOV domain-containing proteins are widespread in all major groups of bacteria (including Archaea), all three major groups of fungi, and all orders of green plants,⁸ the LOV1 and LOV2 domains from phot1 of *Avena sativa* (domestic oats) have served as prototypes for investigating LOV domains from a wide range of organisms.

The structures of several LOV domains have been obtained by X-ray crystallography,⁷ and a solution structure of oat phot1 LOV2 has been obtained by NMR.⁹ These combined studies indicate that LOV domains consist of five antiparallel β sheets separated by short α helices. Downstream of LOV2 is an amphipathic α helix (designated the J- α helix).⁹ This helix is affixed to the β sheets by its hydrophobic side. On photoexcitation of the flavin chromophore, the J- α helix is released from the β sheets and loses its coiled structure, and the structural change presumably activates the downstream kinase moiety in phototropins. Substitution of hydrophilic amino acids on the hydrophobic side of the J- α helix leads to constitutive

Received: January 3, 2014

Published: April 9, 2014

activation of the kinase function.¹⁰ However, this mechanism is not universal. Indeed, the single LOV domain in aureochrome from the stramenopile algae actually activates a bZIP domain that is upstream of the LOV domain, not downstream.¹¹ Hence, photoexcitation of LOV domain proteins can lead to more than one type of conformational change in the protein.

Although much is known about the biochemical and photophysiological properties of the phototropins, progress has been considerably slower in elucidating the post-translational modifications of these photoreceptors. It has been known since the earliest studies that light activates the phosphorylation of multiple sites on a protein¹² that was subsequently identified as phot1.⁶ Salomon et al.¹³ showed that the phosphorylation was in some way hierarchical, with certain sites phosphorylated at low blue light fluences and other sites phosphorylated only at higher blue light fluences. The same study demonstrated the reverse pattern during a period in darkness as the phototropin returned to its dark state after irradiation. More recently, two different studies identified a number of specific sites that become phosphorylated upon light activation.^{14,15} Finally, Roberts et al.¹⁶ demonstrated that phot1 from *Arabidopsis* is monoubiquitinated *in vivo* in response to low fluences of blue light and multi- and/or polyubiquitinated in response to high fluences of blue light.

Any further characterization of the full-length phototropins has been severely hindered by the lack of success in producing sufficient amounts of highly purified photoreceptors for structural, biochemical, or biophysical studies. Here, we use two-dimensional difference gel electrophoresis (2D DIGE) to examine any dynamic changes in mass or charge occurring in full-length *Arabidopsis* phot1 *in vivo* during photoexcitation and subsequent dark recovery. We characterize phot1 in its stable dark state as well as its state immediately after saturating light treatment and the completion of phosphorylation. In addition, we employed a combination of immunoprecipitation and mass spectrometry analysis to search for any additional post-translational modifications that have not been previously identified.

MATERIALS AND METHODS

Plant Materials and Growth Conditions

In this study, *A. thaliana* Columbia (Col-0) seedlings and transgenic *Arabidopsis* expressing phot1-GFP in a *phot1-5* background¹⁷ were used. For etiolated seedlings, seeds were surface-sterilized and sown on MS plates (half-strength MS medium,¹⁸ 0.8% agar, 43.8 mM sucrose, pH 5.7), cold-treated (2 days at 4 °C) in the dark, exposed to white light of medium intensity (100 $\mu\text{mol photons m}^{-2} \text{s}^{-1}$) for 6 h, and then incubated in the dark growth room for 4 days at 22 °C. Blue light irradiation was performed in a growth chamber (E-30 LED, Percival Scientific, Perry, IA, USA) with far-red, red, and blue (468 nm) light-emitting diode sources. The fluence rate was measured using a LI-250A light meter with a LI-190SA quantum sensor (LI-COR, Lincoln, NE, USA). Etiolated seedlings were irradiated for up to 60 min with continuous blue light (20 $\mu\text{mol m}^{-2}$) or left in darkness as controls. The whole seedlings, including the cotyledons, hypocotyls, and roots, were collected and frozen immediately in liquid nitrogen until protein extraction and proteomic analyses were performed (Figure 1).

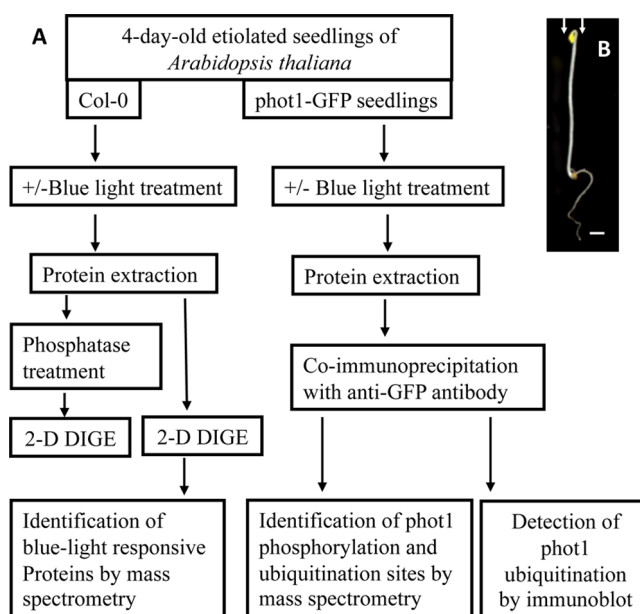


Figure 1. Schematic documentation of the experimental design (A) and a photograph of a representative etiolated *Arabidopsis* seedling (B). Four-day-old etiolated seedlings of *Arabidopsis thaliana* (B) were used and were either left in darkness (control) or irradiated with blue light. Thereafter, entire seedlings were used for protein extraction and proteomic analyses, which were combined with mass spectrometric and immunoblot analyses. Note that blue light treatment was from the top. The white bar is 1 mm in panel B.

Protein Extraction

Microsomal proteins were extracted as described in previous studies.^{19,20} Briefly, liquid-ground tissue powder was mixed with three volumes of extraction buffer (50 mM HEPES, pH 7.5, 0.33 M sucrose, 5% (v/v) glycerol, 3 mM EDTA, and 5 mM DTT) with phosphatase and protease inhibitors (10 mM sodium fluoride, 10 mM sodium molybdate, 10 mM imidazole, 1 mM activated sodium vanadate, 7 μM E-64, 1.5 μM bestatin, 2 μM pepstatin, 4 μM antipain, and 1 mM PMSF) and then centrifuged at 10 000g for 20 min to remove cell debris. The resulting supernatant was centrifuged at 200 000g for 60 min to pellet the microsomal fraction. The microsomal pellet was dissolved in SDS extraction buffer (100 mM Tris-HCl, pH 8.0, 2% SDS, 1% β -mercaptoethanol, 5 mM EGTA, and 10 mM EDTA) and further purified with a modified phenol-methanol protocol as described.²¹ The protein extract was dissolved in 2D DIGE buffer (6 M urea, 2 M thiourea, and 4% CHAPS) and quantified using the Bio-Rad protein assay.

2D DIGE

2D DIGE was performed as described elsewhere.²² Twenty micrograms of microsomal proteins from dark-control or blue light-treated plants (pH 8.5) were mixed with 80 pmol of Cy3 or Cy5 dyes and incubated on ice for at least 2 h in the dark. The labeling reaction was terminated by adding 0.5 μL of 10 mM lysine. Cy3- and Cy5-labeled proteins were then combined and used for isoelectric focusing (IEF). IEF was performed on 24 cm IPG strips, pH 3–10 NL (GE Healthcare, Piscataway, NJ, USA). The running conditions were as follows: rehydration for 2 h, 50 V for 10 h, step and hold at 500 V and then 1000 V for 1 h each, gradient to 8000 V over 3 h, and then at 8000 V until reaching a total of 56 000 V h. Second-dimension electrophoresis was performed using 10% SDS-polyacrylamide

gels. The electrophoresis was performed at 40 V for 2 h and then at 120 V until the bromophenol blue front reached the bottom of the gel. Images of Cy3- and Cy5-labeled proteins were acquired using a Typhoon Trio scanner (GE Healthcare). The estimated pH ranges following IEF are indicated in Figures 2–4.

Image Analysis

DIGE images were analyzed using DeCyder 6.5 software (GE Healthcare). A differential in-gel analysis module with an estimated spot number of 5000 was used for spot detection, and a biological variation analysis module was used to identify spots differentially regulated by blue light (p value < 0.05). Four biological replicates were used in each comparison, and spots of interests were manually checked to confirm spot matching between different gels and to remove artifacts.

Protein Identification Using Mass Spectrometry

Spot picking and reverse-phase liquid chromatography–electrospray tandem mass spectrometry (LC–MS/MS) analyses were performed as follows. Approximately 400 μ g of protein was labeled with 40 pmol of Cy5 dye and separated by 2-DE. After electrophoresis, 2-DE gels were stained with Deep Purple stain (GE Healthcare). Upon scanning the gels with Typhoon Trio, spots of interests were selected with DeCyder software and picked by an Ettan spot picker (GE Healthcare). The excised protein spots were washed twice with 50% acetonitrile in 25 mM ammonium bicarbonate (NH_4HCO_3), vacuum-dried, rehydrated in 10 μ L of digestion buffer (10 ng/ μ L trypsin in 25 mM NH_4HCO_3), and covered with a minimum volume of NH_4HCO_3 .

After overnight digestion at 37 °C, peptides were extracted twice with a solution containing 50% (v/v) acetonitrile and 5% (v/v) formic acid. The extracted digests were vacuum-dried and resuspended in 10 μ L of 0.1% formic acid in water and then analyzed by LC–MS/MS. The digests were separated by nanoflow liquid chromatography using a 100 μ m \times 150 mm reverse-phase Ultra 120 μ m C18Q column (Peeke Scientific, Redwood City, CA, USA) at a flow rate of 350 nL/min in an Agilent 1100 high-performance liquid chromatography system (Agilent Technologies, Inc. Santa Clara, CA, USA). Mobile phase A was 0.1% formic acid in water, and mobile phase B was 0.1% formic acid in acetonitrile. Following equilibration of the column in 2% solvent B, one-half of each digest (5 μ L) was injected, and then the organic content of the mobile phase was increased linearly to 40% over 30 min and then to 50% in 3 min.

The liquid chromatography eluate was coupled to a microionspray source attached to the mass spectrometer. The following mass spectrometers were used for the analysis of the samples: QSTAR Pulsar (Applied Biosystems/MDS Sciex, South San Francisco, CA, USA), QSTAR Elite (Applied Biosystems), LTQ-FT ICR (Thermo Scientific, San Jose, CA, USA), and LTQ Orbitrap XL (Thermo Scientific). Peptides were analyzed in positive ion mode and in information-dependent acquisition mode to switch automatically between MS and MS/MS acquisition. For experiments using the QSTAR Pulsar and QSTAR Elite, MS spectra were acquired for 1 s in the m/z range between 310 and 1400. MS acquisitions were followed by 3 s collision-induced dissociation (CID) experiments in information-dependent acquisition mode. For each MS spectrum, the most intense multiply charged peaks over a threshold of 30 counts were selected for generation of CID mass spectra. The CID collision energy was

automatically set according to the mass-to-charge (m/z) ratio and charge state of the precursor ion. A dynamic exclusion window was applied that prevented the same m/z from being selected for 60 s after its acquisition. For experiments using the LTQ Orbitrap XL and LTQ FT ICR, MS spectra were acquired in profile mode using the Orbitrap or ICR analyzers in the m/z range between 310 and 1600. For each MS spectrum, the six most intense multiply charged ions over a threshold of 400 counts were selected to perform CID experiments. Product ions were analyzed on the linear ion trap in profile mode. CID collision energy was automatically set to 35%. A dynamic exclusion window of 1 Da was applied that prevented the same m/z from being selected for 60 s after its acquisition.

Peak lists from files acquired by the QSTAR instruments were generated using Mascot Distiller version 2.1.0.0 (Matrix Science, Boston, MA, USA). Parameters for MS processing were set as follows: peak half-width, 0.02; data points per dalton, 100. Parameters for MS/MS data were set as follows: peak half-width, 0.02; data points per dalton, 100. In the case of data acquired in the LTQ Orbitrap XL and LTQ FT Thermo Scientific instruments, peak lists were generated using PAVA in-house software,²³ which is based on the RawExtract script from Xcalibur v2.4 (Thermo Fisher Scientific). In all cases, the peak lists were searched in-house using ProteinProspector version 5.4.2²⁴ (the public version is available at <http://prospector.ucsf.edu>). The enzyme specificity was set to trypsin, and the maximum number of missed enzyme cleavages per peptide was set at one. The number of modifications was limited to two per peptide. Carbamidomethylation of cysteine was included as a fixed modification; N-acetylation of the N terminus of the protein, oxidation of methionine, formation of pyro-Glu from N-terminal glutamine, phosphorylation of serine, threonine, or tyrosine, and ubiquitination of lysine were all allowed as variable modifications. In searches of LTQ-Orbitrap XL or LTQ-FT data, the mass tolerance was 30 ppm for precursor and 0.8 Da for fragment ions. For QSTAR data, a precursor mass tolerance of 100 ppm and a fragment mass error tolerance of 0.2 Da were allowed for the data search.

The peak lists were searched against a subset of the UniProtKB database as of December 15, 2009, containing all entries for *Arabidopsis* (53 624 entries searched). The false positive rate was estimated by searching the data using a concatenated database that contains the original *Arabidopsis* UniProtKB database as well as a version of each original entry where the sequence was randomized. In all protein identifications, a minimal protein score of 22, a peptide score of 15, and a minimal discriminate score threshold of 0.0 were used for initial identification criteria. The maximum expectation value threshold (number of different peptides with scores equivalent to or better than the result reported that are expected to occur in the database search by chance) was set to 0.05 for accepting individual spectra and 0.01 for accepting individual proteins. When several accession numbers in the database corresponding to overlapping sequences of the same polypeptide were identified, the common gene locus and protein name were reported. Only proteins with at least two peptides identified were further considered and reported. To assign the modification site for peptides containing post-translational modifications, the MS/MS spectrum was reinterpreted manually by matching the observed fragment ions to a theoretical fragmentation obtained using MS Product (ProteinProspector).

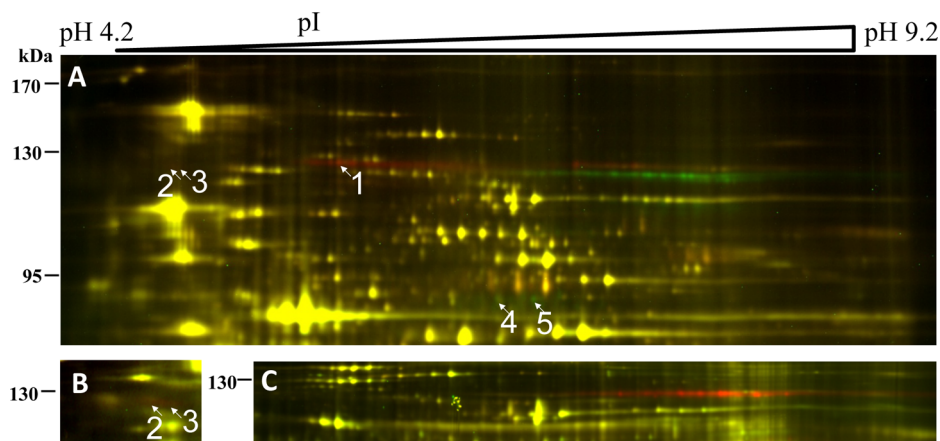


Figure 2. 2D DIGE analysis of the blue light response in the microsomal fraction of 4 day old etiolated *Arabidopsis* seedlings. (A, B) Col-0 seedlings were irradiated with blue light for 20 min, and microsomal proteins from both control (unirradiated, proteins labeled with Cy3) and irradiated seedlings (proteins labeled with Cy5) were analyzed by 2D DIGE. (A) Superimposed 2D DIGE image of the upper-half of a gel. Proteins (in different modification isoforms) induced by blue light treatment appear as red spots, and those decreased by the treatment appear green, whereas those remaining constant appear yellow. Spots that were characterized by mass spectrometry are highlighted by arrows, and their identities are listed in Table 1. (B) Zoomed-in 2D DIGE overlay image (from a different gel than that in panel A) showing the blue light-stimulated accumulation of WEB1 in the microsomal fraction. (C) Identities of the row of phot1 spots were further confirmed by 2D DIGE analysis of the microsomal protein of the etiolated seedlings of the *phot1-5* (labeled with Cy3, green) and *gl* (its genetic background, labeled with Cy5, red) mutants. The estimated pH ranges following IEF are indicated above the gel images in Figures 2–4.

Table 1. 2D DIGE Identified phot1 and WEB1 as Blue Light-Responsive Proteins in *Arabidopsis*^a

spot	gene locus	protein name	abundance ratio	<i>p</i> value (<i>t</i> test)	unique peptides	sequence coverage (%)	E value
1	At2g42600	phot1	3.22	0.0006	13	22.6	1.3×10^{-7}
2	At2g26570	WEB1	1.29	0.008	12	17.1	7.2×10^{-6}
3	At2g26570	WEB1	1.29	0.008	19	25.2	6.6×10^{-5}
4	At2g42600	phot1	-1.38	0.047	4	4.5	0.0022
5	At2g42600	phot1	-1.27	0.026	11	12.4	6.6×10^{-5}

^aAs shown in Figure 2A, proteins spots responsive to blue light were screened by DeCyder software and were further characterized by MS/MS. The spot volume ratios of blue light-irradiated to untreated (positive numbers) or untreated to irradiated (negative numbers) and the *p* values of the Student's *t*-test of the comparison were calculated from three biological replicates. For the MS/MS identification, the number of unique peptides, percentage of sequence coverage, and E value (best expectation value) for each spot are listed.

Phosphatase Treatment

Phosphatase treatment was performed as described elsewhere.^{25,26} In brief, 50 μ L of microsomal protein (approximately 250 μ g) in DIGE buffer was mixed with 5 μ L of 10% SDS. Then, 345 μ L of deionized water, 50 μ L of 20 mM MnCl₂, and 50 μ L of 10 \times λ -protein phosphatase buffer were added sequentially, mixed, and incubated with 200 units of λ -protein phosphatase enzyme (New England Biolabs, Ipswich, MA, USA) overnight at 30 $^{\circ}$ C. Then, proteins were pelleted by adding five volumes of 0.1 M ammonium acetate in methanol and dissolved in DIGE buffer.

Co-Immunoprecipitation and Immunoblot

Co-immunoprecipitations were performed as described by Kim et al.²⁷ The microsomal proteins were prepared as described above and were resuspended in the extraction buffer containing 0.1% (w/v) Triton X-100. After centrifugation at 20 000g for 10 min, solubilized proteins were incubated with an anti-GFP antibody bound to protein A Sepharose beads (GE Healthcare) for 1 h. The beads were washed four times with the extraction buffer containing 0.1% Triton X-100 and eluted with 2% SDS.

Microsomal proteins and the immunoprecipitated proteins were resolved on 7.5% SDS-PAGE gel, transferred to a nitrocellulose membrane, and then stained with Deep Purple stain (GE Healthcare), as described.²¹ Ubiquitination of phot1 was detected by western blot using an anti-ubiquitin antibody

(FK2, mouse monoclonal, Enzo Life Science, Farmingdale, NY, USA), which detects both mono- and polyubiquitinated proteins.

RESULTS

Identification of Blue Light-Responsive Proteins

Blue light acts as an environmental cue to regulate plant growth and development, but its perception and transduction by plants remains poorly characterized. To understand better the early events of blue light signaling, the experimental protocol illustrated in Figure 1 was employed to study the effect of blue light on the proteome of *Arabidopsis* seedlings. Here, we used 2D DIGE coupled with tandem mass spectrometry to identify early blue light-responsive proteins and protein modifications. Four-day-old etiolated seedlings were irradiated with blue light at a fluence rate of 20 μ mol m⁻² s⁻¹ for 20 min, a total fluence that is known to saturate the phosphorylation of phot1.^{12,28} Because blue light-induced phototropism is initiated by membrane-associated receptors phot1 and phot2, crude membrane proteins (microsomal fraction) from blue light-irradiated and unirradiated seedlings were compared by 2D DIGE. Two rows of high-molecular-weight proteins (approximately 120 kDa) showed clear mobility shifts in which the more acidic ones showed up only after irradiation and exhibited slightly lower electrophoretic mobility, whereas the more basic

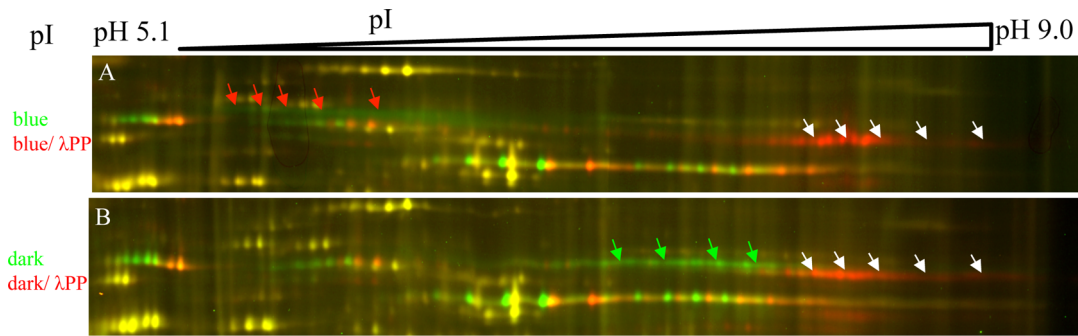


Figure 3. Phosphorylation is the major form of phot1 post-translational modification, as indicated by λ -phosphatase treatment. Phosphatase treatment induced shifts of phot1 spots in microsomal protein from both blue light-irradiated (A) and control (B) seedlings. On the left, “blue and blue/ λ PP” indicates the comparison of phosphatase-treated (cy5, red) versus untreated (cy3, green) microsomal proteins from blue light-irradiated seedlings by 2D DIGE and “dark and dark/ λ PP” indicates the comparison of phosphatase treated (cy5, red) versus untreated (cy3, green) proteins from unirradiated seedlings. Proteins that show up in the phosphatase-treated samples appear red, whereas those in the untreated samples are green. Red arrows point to phot1 spots from samples of irradiated seedlings, green arrows point to those from the unirradiated samples, and white arrows point to those from phosphatase-treated proteins.

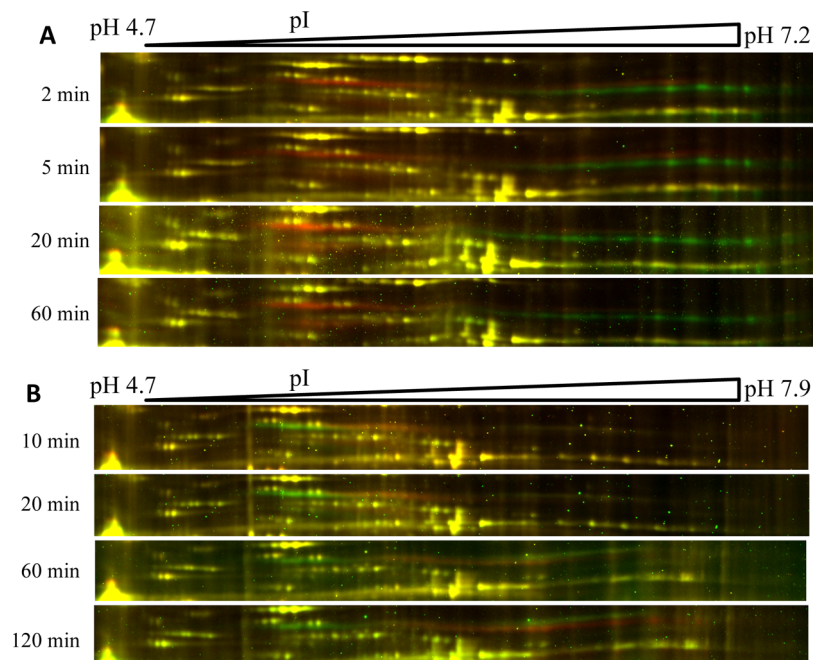


Figure 4. Time-dependent phot1 phosphorylation (A) and dephosphorylation (B) after irradiation of dark-grown seedlings. (A) Etiolated Col-0 seedlings were irradiated with blue light for the indicated times, and the microsomal proteins from irradiated (red) and unirradiated samples (green) were compared by 2D DIGE. Shown are the overlay images containing the phot1 region. (B) After saturating irradiation for 20 min, the etiolated seedlings were kept in the dark. The subsequent phot1 dephosphorylation was monitored by 2D DIGE, comparing the microsomal protein from the Col-0 seedling collected at the time points indicated with that of the control samples (collected immediately after irradiation).

ones disappeared after irradiation (Figure 2A), which is the pattern that one would expect to see for light-induced protein phosphorylation.

In-gel trypsin digestion of an excised spot followed by liquid chromatography–tandem mass spectrometry (MS/MS) identified these spots as phot1 (Figure 2A, arrow 1, and Table 1), a result that was expected because phot1 has an apparent size of 120 kDa.^{6,29} The identities of the row of phot1 spots from the unilluminated control seedlings were further confirmed by 2D DIGE comparison of *phot1-5* with its genetic background, *gl*, as these spots disappeared in the *phot1-5* mutant (Figure 2C). Two other blue light-responsive protein spots with higher electrophoretic mobility were also identified as phot1 (Figure 2A, arrows 4 and 5), which are likely the partial degradation products of phot1. In addition to phot1, a blue light-responsive

protein was identified as WEB1 (weak chloroplast movement under blue light 1, Figure 2, arrows 2 and 3), an acidic high-molecular-weight protein regulating the movement velocity of chloroplast photorelocation.³⁰ WEB1 was previously shown to be predominantly in the soluble fraction of the proteome, with only a little found in the microsomal fractions.³⁰ This is in agreement with its low abundance in the microsomal fraction in our study (Figure 2B). The accumulation of WEB1 protein in the microsomal fraction after blue light irradiation suggests that light induces WEB1 association with the cell membrane or some other cellular structure.

Differential Phosphorylation of phot1

The two rows of phot1 spots extended from the basic to the acidic region in the gel shown in Figure 2A. To determine

whether all of these spots are the result of differential phosphorylation of phot1, λ -protein phosphatase treatment, which hydrolyzes the phosphate groups from serine, threonine, tyrosine, and histidine residues, was performed on the microsomal proteins from both dark and blue light-irradiated seedlings. In both cases, phosphatase treatment shifted phot1 to the more basic regions and increased its electrophoretic mobility (Figure 3A,B). However, phot1 was still found as a string of spots in the 2-DE gels after the phosphatase treatment, possibly the result of incomplete phosphatase digestion and/or post-translational modifications other than phosphorylation (i.e., any modifications affecting charge of the protein).

Salomon et al.¹³ found that the phosphorylation of phot1 in *Avena sativa* was, in some way, hierarchical, with certain sites phosphorylated at low blue light fluences and other sites phosphorylated at higher blue light fluences. We applied 2D DIGE to study the time-dependent phot1 phosphorylation and dephosphorylation patterns in *Arabidopsis*. As shown in Figure 4A, a 2 min irradiation at a fluence rate of 20 $\mu\text{mol m}^{-2}$ stimulated phot1 phosphorylation, as indicated by the acidic shift. A 5 min irradiation shifted phot1 further to the more acidic regions and appeared to saturate phot1 phosphorylation, as longer time treatment (20 and 60 min, respectively) did not cause any further spot shifts in the acidic regions. In contrast, dephosphorylation of phot1 in a sequential order was observed when the saturation-illuminated (20 min) seedlings were kept in the dark. After a 10 min recovery period in darkness, the charges in phot1 were shifted partially toward a more basic pI, as shown on the 2D DIGE gel, and after 60 min, there were no further shifts in electrophoretic mobility.

Identification of Novel in Vivo phot1 Phosphorylation Sites

Two previous studies identified eight different in vivo phot1 phosphorylation sites,^{14,15} but the large number of phot1 spots with distinct pI values (Figures 2–4) that were shifted by protein phosphatase treatment (Figure 3) suggested the existence of additional phot1 phosphorylation sites. To identify other possible phot1 phosphorylation sites, an anti-GFP antibody was used to immunoprecipitate phot1-GFP from the microsomal proteins of both irradiated and unirradiated *Arabidopsis* seedlings expressing phot1-GFP,¹⁷ and the immunoprecipitates were analyzed by tandem mass spectrometry after separation by SDS-PAGE. In the phot1-GFP proteins from dark-grown seedlings, three phosphorylated Ser sites were observed (Supporting Information Figure 1), with all of them located in the N-terminus (Figure 5). In the illuminated samples, 13 phosphorylation sites were identified (Figure 5 and Supporting Information Figure 1), which were localized both to the N-terminus and the hinge region between LOV1 and LOV2 (Figure 5), including two sites (S58 and S170) that were also detected in the dark sample. A representative annotated tandem mass spectrum of phot1 phosphopeptides is shown in Figure 6 (for the identity of the phosphorylation sites, see Table 2). In all, we report 14 distinct Ser/Thr residues phosphorylated in vivo. Because six of the sites (S58, S170, S185, S350, S376, and S410) were reported to be phosphorylated in vivo either in the dark or in illuminated samples,^{14,15} we report here eight additional in vivo phosphorylated sites (indicated in red in Figure 5).

In a similar study, Inoue et al. identified 25 phosphorylated Ser/Thr residues in *Arabidopsis* phot2 by LC-MS/MS.³¹ These sites are located both in the N-terminus and Hinge-1 regions. Interestingly, sequence alignment showed that S185

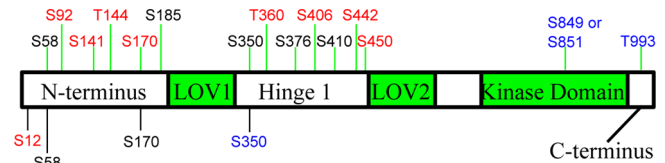


Figure 5. Summary of known phot1 phosphorylation sites. Phosphorylated Ser/Thr sites identified from blue light-treated tissues are shown above the protein box, whereas those identified from the dark tissues are shown below the protein box. Ser/Thr sites in black were identified both in this study and in previous studies,^{14,15} those in blue were not identified in this study but were reported previously, and those in red are new sites identified in this study. Phosphorylated S170 was identified from phot1 protein in both dark and irradiated seedlings in this study, but it was identified only from phot1 protein in dark seedlings in a previous study.¹⁵ In summary, eight new unique sites (S12, S92, S141, T144, T360, S406, S442, and S450) were identified in this study.

(in phot1) or S121 (in phot2), located in a highly conserved amino acid region just before LOV1 domain of phot1/2, is the only known conserved site phosphorylated in both proteins in vivo (Supporting Information Figure 2).

Ubiquitination of phot1

Ubiquitination of phot1 has been shown to be involved in phototropic responses,¹⁶ but the ubiquitination site(s) of phot1 have not yet been characterized. Key features for detection of potential ubiquitin attachment sites on tryptic peptides are the missed cleavage of the modified lysine together with a shift of 114 Da (a diglycine moiety, GG) in both the mass of the precursor ion and the masses of sequence fragment ions in the MS/MS spectrum that would contain the ubiquitin-modified site of the peptide.^{32,33} These GG remnants result from the cleavage by trypsin of the original ubiquitin in the C-terminal side or R on its C-terminal GGR sequence.³³ Accordingly, a unique ubiquitination site (K526), localized in the LOV2 region, was observed in the spectrum of the peptide F514–K527 of phot1-GFP from blue light-irradiated seedlings (Figure 7), but it was not observed in the dark controls (data not shown). To document that ubiquitination of phot1 was regulated by blue light irradiation, phot1-GFP proteins immunoprecipitated by an anti-GFP antibody were immunoblotted with an anti-ubiquitin FK2 antibody that detects both mono- and polyubiquitinated proteins. Immunoblot assays show that phot1 ubiquitination was enhanced after blue light irradiation, whereas it was reduced during recovery in the dark, in a pattern similar to that of phot1 phosphorylation (Figure 8).

DISCUSSION

Crop yield is, to a large extent, dependent on the photosynthetic activity of the green leaves of the developing plant. Recent studies have shown that the photosynthetic efficiency of these organs is optimized via a number of blue light/UV-A-mediated responses, such as phototropism in the upper region of the plant, chloroplast movement, stomatal opening, palisade cell development, and leaf flattening.^{3,4} In the model organism *A. thaliana*, all of these physiological processes are mediated by phototropins (phot1 and phot2), as reviewed by Christie et al.³ However, the signaling cascade that leads from the photoexcitation of phot1 (or phot2) to the corresponding physiological response has not yet been elucidated in detail. The aim of this study was to explore this signaling pathway in *Arabidopsis* further. We detected the phosphorylation of phot1

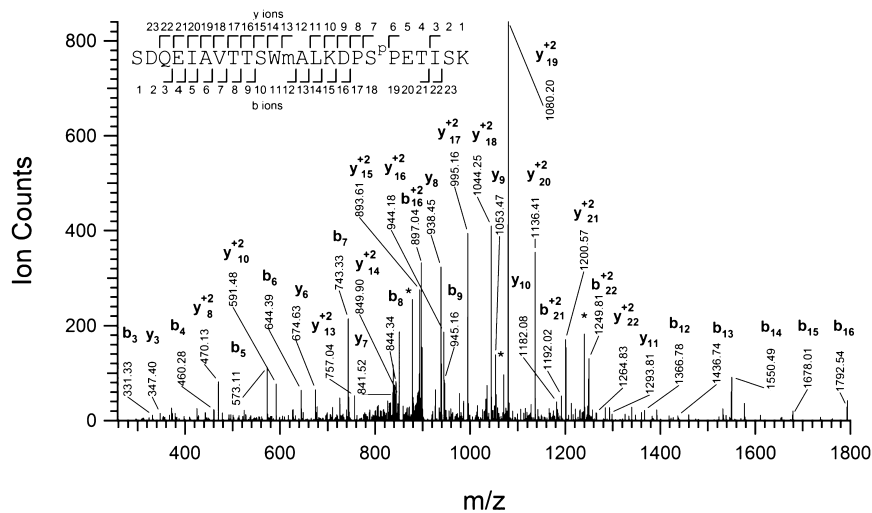


Figure 6. Representative CID MS/MS spectrum of phot1 obtained from a precursor ion with a m/z value of 910.7604⁺³, corresponding to a phosphorylated peptide spanning the residues S75–K98 of phot1 (theoretical monoisotopic mass value, 910.7576⁺³; error in the mass observed in the precursor ion, 3.1 ppm). Phosphorylated serine is shown in the sequence as S^P. The observed b and y product ion peaks are labeled accordingly, with the subscripts denoting their position in the identified peptide. Intense ions corresponding to neutral losses from the labeled sequence ions are indicated by *. In the peptide sequence, m denotes oxidized methionine.

Table 2. Identification of in Vivo Phosphorylation Sites of Immunoprecipitated phot1–GFP by LC–MS/MS^a

sample	sequence	mass precursor	charge state	error (ppm)	modified residue	E value	instrument
blue	GTS*PQPRPQQEPAPSNPVR	708.3476	3	12	S58	1.10 × 10 ⁻⁵	Orbitrap
blue	SDQEIAVTTSwmALKDPS*PETISK	910.7604	3	3.1	S92	1.20 × 10 ⁻⁴	Orbitrap
blue	TGKPGQGVGRNS*GGTENDPNGK	750.3483	3	-0.12	S141	0.0032	Orbitrap
blue	TGKPGQGVGRNS*GGT*ENDPNGK	777.0049	3	1.4	S141, T144	0.034	Orbitrap
blue	SSGEmS*DGDPVGGGR	723.7649	2	1.5	S170	4.30 × 10 ⁻⁴	Orbitrap
blue	SGIPRVS*EDLK	640.8157	2	-0.38	S185	0.0022	Orbitrap
blue	ALS*ESTNLHPFmTK	557.9237	3	-0.73	S350	6.80 × 10 ⁻⁷	Orbitrap
blue	ALSESTNLHPFmT*KSEDELPK	853.055	3	-0.95	T360	2.10 × 10 ⁻⁴	Orbitrap
blue	RmS*ENVVPSGR	443.2065	3	17	S376	5.50 × 10 ⁻⁴	QStar Elite
blue	INEIPEKKS*R	647.3313	2	-0.77	S406	0.016	Orbitrap
blue	KSS*LSFmGIK	597.2902	2	8.1	S410	3.60 × 10 ⁻⁸	QStar Elite
blue	SESLDESIDDGFIEYGEEDEIS*DRDERPESVDDK	1372.2279	3	3	S442	0.004	Orbitrap
blue	DERPES*VDDK	635.2542	2	1.4	S450	0.0097	Orbitrap
blue	SESLDESIDDGFIEYGEEDEIS*DRDERPES*VDDKVR	1483.9426	3	4.6	S442, S450	0.022	Orbitrap
dark	Acetyl-mMEPTEKPKS*SRTLPR	727.3506	3	-2	S12	0.046	Orbitrap
dark	GTS*PQPRPQQEPAPSNPVR	708.3375	3	-2.3	S58	5.10 × 10 ⁻⁵	Orbitrap
dark	SSGEmS*DGDPVGGGR	723.7642	2	0.54	S170	0.011	Orbitrap

^aFigure 5 shows a scheme illustrating the 16 sites along the phot1 protein. Mass spectra for peptides in this table are provided in Figure 6 and in Supporting Information Figure I. S* and T* represent phosphorylation sites. m represents oxidized methionine.

and accumulation of WEB1 in the membrane-associated protein fraction by 2D DIGE (Figures 2–4), and we identified a large number of phot1 Ser/Thr sites phosphorylated in vivo (Figure 5) as well as a phot1 ubiquitination site, which was identified by mass spectrometry analysis of phot1–GFP co-immunoprecipitates (Figure 7). These results further revealed the complexity of phot1 post-translational modifications.

Since phototropins were first found to be membrane-associated proteins that are phosphorylated upon blue light irradiation in etiolated seedlings of pea (*Pisum sativum*),³⁴ much progress has been made in characterizing the phosphorylation of phototropins. Salomon et al.¹³ identified eight Ser residues in oat phot1a in vitro that are phosphorylated, which are hierarchically located either in the N-terminus or Hinge 1 region. Sullivan et al.¹⁵ identified four phosphorylation sites in vivo in *Arabidopsis* phot1: two in the N-terminus and two in the

Hinge 1 region. Inoue et al.¹⁴ identified eight Ser/Thr residues in *Arabidopsis* phot1, including one in the kinase domain and one in the C-terminus (that we did not detect) in addition to six in the N-terminus or Hinge 1 region. Interestingly, all the four sites identified by Sullivan et al.¹⁵ were observed by Inoue et al.¹⁴ However, the large number of individual protein spots (over 50) from the two rows of phot1 spanning from the basic to the acidic regions detected in our 2D DIGE gels (Figure 2A) indicates the greater complexity of phot1 phosphorylation. Our study identified 14 discrete Ser/Thr sites phosphorylated in vivo, which included six sites identified by Sullivan et al.¹⁵ and Inoue et al.¹⁴ (Figure 5). In addition, we identified eight additional Ser/Thr sites phosphorylated in vivo from unirradiated and blue light-exposed samples. A string of parallel phot1 spots was detected in the unirradiated etiolated samples (Figure 2A,C), and they were shifted to more basic regions

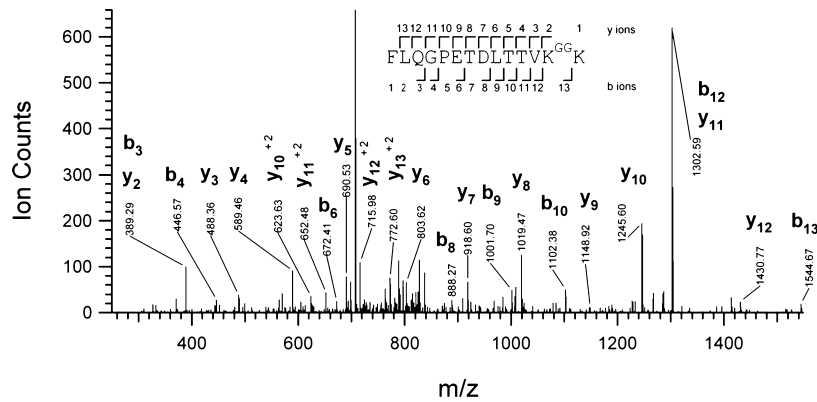


Figure 7. CID MS/MS spectrum obtained from a precursor ion with a m/z value of 845.9529^{+2} , corresponding to a ubiquitinated peptide spanning residues F514–K527 of phot1 (theoretical monoisotopic mass value, 845.9542^{+2} ; error in the mass observed in the precursor ion, -1.4 ppm). Ubiquitinated lysine is shown in the sequence as K^{GG} , as it is labeled by the diGly tryptic remnant of ubiquitin. The observed sequence ions are displayed.

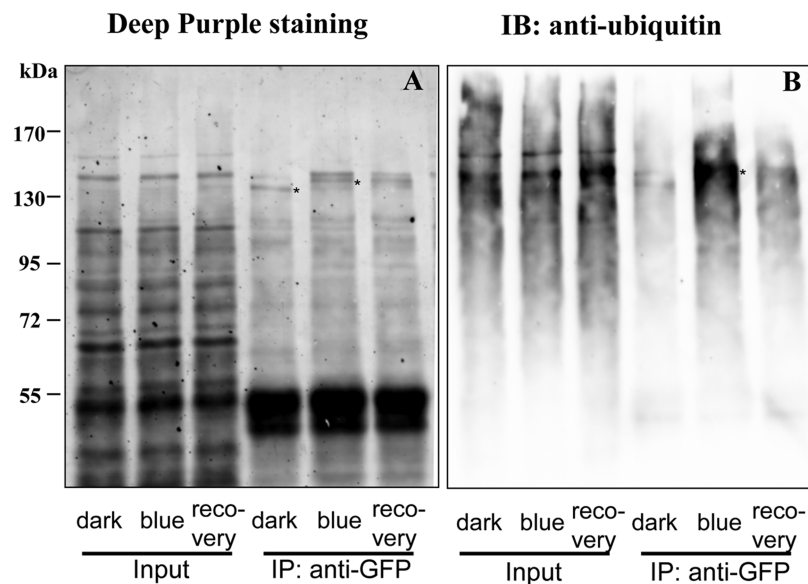


Figure 8. Ubiquitination of phot1–GFP is regulated by blue light. *Arabidopsis* seedlings expressing phot1–GFP were grown in the dark for 4 days. Thereafter, one-third of the samples were collected immediately under dim safe light (dark), another third were irradiated with blue light for 20 min (blue), and the remaining seedlings were incubated in the dark for 60 min after 20 min of blue light irradiation (recovery). Microsomal proteins were extracted from these seedlings and immunoprecipitated with an anti-GFP antibody. The microsomal proteins (input) and the immunoprecipitates (IP; anti-GFP) were resolved by a 7.5% SDS–PAGE gel, transferred to a nitrocellulose membrane, stained by Deep Purple fluorescent stain (A), and detected by an anti-ubiquitin antibody (B). In panel A, phot1–GFP with lower and higher electrophoretic mobilities is marked with stars. In panel B, ubiquitination of phot1 is marked with a star.

after phosphatase treatment, indicating that some sites of phot1 were phosphorylated even in the dark. In this study, we identified three such phosphoserine residues from phot1 in seedlings without blue light treatment (Figure 5).

Despite the large number of phosphorylation sites identified for phototropins in this and other studies, there are only a few reports of their possible function. Kinoshita et al. reported the binding of a 14-3-3 protein to S358 in *Vicia faba* phot1a and S344 in *V. faba* phot1b and proposed that the binding is likely a key step in the phototropin-mediated stomatal opening response.³⁵ Sullivan et al. report the binding of a 14-3-3 protein to S350 and S376 of *Arabidopsis* phot1; because S376 corresponds to S344 in *V. faba* phot1b,¹⁵ it could possibly serve the same role. Inoue et al. showed that autophosphorylation of S851 in the kinase activation loop was essential for a whole series of phot1-mediated responses in *Arabidopsis* and proposed

a possible secondary role for S849.¹⁴ Finally, Tseng et al. demonstrated that S747 in *Arabidopsis* phot2 bound the λ isoform of a 14-3-3 protein in a yeast two-hybrid screen and that mutating that serine to alanine blocked phot2-mediated stomatal opening.³⁶ The mutation failed to have an impact on phototropism, however, indicating a high level of specificity. Sorting out the roles of the many phototropin phosphorylations remains a daunting task.

A string of protein spots was observed in the phot1 region in the microsomal protein samples from either the unirradiated or irradiated seedlings, even after overnight phosphatase treatment of the microsomal proteins, suggesting additional post-translational modifications other than phosphorylation and/or incomplete phosphatase treatment. In addition to protein phosphorylation, ubiquitination is another important post-translational modification that regulates protein activity,

including protein degradation, membrane protein endocytosis, and subcellular protein trafficking.^{37–39} Roberts et al.¹⁶ showed that phot1 could be mono-, multi-, or polyubiquitinated, depending on light intensity, and phot1-interacting protein nonphototropic hypocotyl 3 (NPH3) functions as a substrate adaptor in an E3 Cullin3-based ubiquitin ligase. They also showed that their high-intensity light treatment failed to induce any detectable ubiquitination *in vivo* in an *nph3* mutant, indicating that NPH3 is involved in the ubiquitination that we detected.

Our study showed that Lys526 is likely to be the site of ubiquitination. In addition, we found that ubiquitination of phot1 followed a pattern similar to that for phosphorylation: both increased after blue light exposure but subsequently decreased during the recovery stage following a saturating light exposure. It seems likely that ubiquitination in addition to phosphorylation could account for the increase in mass that we detected for phot1 on illumination *in vivo*. Lys526 is very close to the attachment of the J- α helix to the LOV2 domain, so it is reasonable to expect that it could affect LOV domain unfolding following photoexcitation or folding during dark recovery. In this manner, it could actually play a role in modulating physiological responses. A tryptophan, W491, is also extremely close to lys526, and Hoersch et al.⁴⁰ presented evidence that this tryptophan is moved into a more hydrophilic environment upon LOV domain photoexcitation, indicative of the protein conformational changes in this region of the molecule.

Because they are unstable, of low abundance, and often in low stoichiometry, phosphopeptides are hard to detect by mass spectrometry alone, and immunoprecipitation or other methods are often used to enrich specific proteins to identify phosphopeptides. Even so, only a small number of phosphopeptides has been previously identified for phot1.^{14,15} However, 2D DIGE, which separates two or three samples in the same gel, can detect slight differences in pI as a result of a change in phosphorylation at any residue of the protein. Therefore, the shifted spots in 2D DIGE provide a more accurate estimate of protein phosphorylation sites.⁴¹ As shown before, 2-DE gels resolved over 20 spots of the brassinosteroid-signaling transcription factor BZR1, which is consistent with the number of phosphorylation sites predicted on the basis of the consensus substrate sequence for the BIN2/GSK3 kinase.⁴² Only with the combination of protein fractionation and enrichment, tandem mass spectrometry, and 2D DIGE can a more accurate picture of specific protein phosphorylation and dephosphorylation be elucidated.

Our study and previous studies showed that more than 16 phosphorylation sites and a number of other post-translationally modified residues affecting charge are likely present for phot1. Further studies will be required to characterize the biochemical complexity of the phot1 protein and its physiological implications. Except for the phosphorylation sites in the kinase domain,^{13,14,34} the function of other phosphorylation sites is not known for phototropin-mediated signaling, but it might be expected to play some role in one or more blue light-induced physiological responses.¹⁵

■ ASSOCIATED CONTENT

● Supporting Information

Annotated mass-labeled spectra for the phosphorylated peptides shown in Table 2 and amino acid alignment of the N-terminal and Hinge 1 regions of phototropins from

Arabidopsis thaliana (Atphot1 and Atphot2), *Vicia faba* (Vfphot1a and Vfphot1b), *Oryza sativa* (Osphot1 and Osphot2), and *Avena sativa* (Asphot1a). This material is available free of charge via the Internet at <http://pubs.acs.org>.

■ AUTHOR INFORMATION

Corresponding Author

*Tel.: 1-650-3251521; Fax: 1-650-3256857; E-mail: zywang24@stanford.edu.

Author Contributions

[†]Z.D. and J.A.O.-P. contributed equally to this work.

Notes

The authors declare no competing financial interest.

■ ACKNOWLEDGMENTS

This project was supported by the National Science Foundation (grant 0843617 to W.R.B.); the Ministry of Science and Technology of China (973 program grant 2013CB127101 to Z.D.) and Zhejiang Natural Science Foundation (grant LR12C02002 to Z.D.); the Division of Chemical Sciences, Geosciences, and Biosciences, Office of Basic Energy Sciences of the U.S. Department of Energy (grant DE-FG02-08ER15973); the National Institutes of Health (grant R01GM066258 to Z.-Y.W. and A.L.B.); and the Alexander von Humboldt-Foundation, Bonn, Germany (AvH-Fellowships Stanford 2008–2012 to U.K., University of Kassel, Germany). Mass spectrometry analysis was performed by the Bio-Organic Biomedical Mass Spectrometry Resource at UCSF (A. L. Burlingame, Director) supported by the Biomedical Research Technology Program of the NIH National Center for Research Resources, NIH NIGMS (grants 8P41GM103481 and 1S10RR019934).

■ REFERENCES

- (1) Chen, M.; Chory, J.; Fankhauser, C. Light signal transduction in higher plants. *Annu. Rev. Genet.* **2004**, *38*, 87–117.
- (2) Moglich, A.; Yang, X.; Ayers, R. A.; Moffat, K. Structure and function of plant photoreceptors. *Annu. Rev. Plant Biol.* **2010**, *61*, 21–47.
- (3) Christie, J. M. Phototropin blue-light receptors. *Annu. Rev. Plant Biol.* **2007**, *58*, 21–45.
- (4) Inoue, S.; Kinoshita, T.; Takemiya, A.; Doi, M.; Shimazaki, K. Leaf positioning of *Arabidopsis* in response to blue light. *Mol. Plant* **2008**, *1*, 15–26.
- (5) Briggs, W. R.; Christie, J. M. Phototropins 1 and 2: Versatile plant blue-light receptors. *Trends Plant Sci.* **2002**, *7*, 204–210.
- (6) Christie, J. M.; Raymond, P.; Powell, G. K.; Bernasconi, P.; Raibekas, A. A.; Liscum, E.; Briggs, W. R. *Arabidopsis* NPH1: A flavoprotein with the properties of a photoreceptor for phototropism. *Science* **1998**, *282*, 1698–1701.
- (7) Losi, A.; Gartner, W. The evolution of flavin-binding photoreceptors: An ancient chromophore serving trendy blue-light sensors. *Annu. Rev. Plant Biol.* **2012**, *63*, 49–72.
- (8) Krauss, U.; Minh, B. Q.; Losi, A.; Gartner, W.; Eggert, T.; von Haeseler, A.; Jaeger, K. E. Distribution and phylogeny of light-oxygen-voltage-blue-light-signaling proteins in the three kingdoms of life. *J. Bacteriol.* **2009**, *191*, 7234–7242.
- (9) Harper, S. M.; Neil, L. C.; Gardner, K. H. Structural basis of a phototropin light switch. *Science* **2003**, *301*, 1541–1544.
- (10) Harper, S. M.; Christie, J. M.; Gardner, K. H. Disruption of the LOV-J α helix interaction activates phototropin kinase activity. *Biochemistry* **2004**, *43*, 16184–16192.
- (11) Takahashi, F.; Yamagata, D.; Ishikawa, M.; Fukamatsu, Y.; Ogura, Y.; Kasahara, M.; Kiyosue, T.; Kikuyama, M.; Wada, M.;

- Kataoka, H. AUREOCHROME, a photoreceptor required for photomorphogenesis in stramenopiles. *Proc. Natl. Acad. Sci. U.S.A.* **2007**, *104*, 19625–19630.
- (12) Short, T. W.; Briggs, W. R. Characterization of a rapid, blue light-mediated change in detectable phosphorylation of a plasma membrane protein from etiolated pea (*Pisum sativum* L.) seedlings. *Plant Physiol.* **1990**, *92*, 179–85.
- (13) Salomon, M.; Knieb, E.; Von Zeppelin, T.; Rudiger, W. Mapping of low- and high-fluence autophosphorylation sites in phototropin 1. *Biochemistry* **2003**, *42*, 4217–4225.
- (14) Inoue, S.; Kinoshita, T.; Matsumoto, M.; Nakayama, K. I.; Doi, M.; Shimazaki, K. Blue light-induced autophosphorylation of phototropin is a primary step for signaling. *Proc. Natl. Acad. Sci. U.S.A.* **2008**, *105*, 5626–5631.
- (15) Sullivan, S.; Thomson, C. E.; Lamont, D. J.; Jones, M. A.; Christie, J. M. In vivo phosphorylation site mapping and functional characterization of *Arabidopsis* phototropin 1. *Mol. Plant* **2008**, *1*, 178–194.
- (16) Roberts, D.; Pedmale, U. V.; Morrow, J.; Sachdev, S.; Lechner, E.; Tang, X.; Zheng, N.; Hannink, M.; Genschik, P.; Liscum, E. Modulation of phototropic responsiveness in *Arabidopsis* through ubiquitination of phototropin 1 by the CUL3-Ring E3 ubiquitin ligase CRL3(NPH3). *Plant Cell* **2011**, *23*, 3627–3640.
- (17) Sakamoto, K.; Briggs, W. R. Cellular and subcellular localization of phototropin 1. *Plant Cell* **2002**, *14*, 1723–1735.
- (18) Murashige, T.; Skoog, F. A revised medium for rapid growth and bio-assays with tobacco tissue cultures. *Physiol. Plant.* **1962**, *15*, 473–497.
- (19) Kutschera, U.; Deng, Z.; Osés-Prieto, J. A.; Burlingame, A. L.; Wang, Z. Y. Cessation of coleoptile elongation and loss of auxin sensitivity in developing rye seedlings: A quantitative proteomic analysis. *Plant Signaling Behav.* **2010**, *5*, 509–517.
- (20) Li, T.; Xu, S. L.; Osés-Prieto, J. A.; Putil, S.; Xu, P.; Wang, R. J.; Li, K. H.; Maltby, D. A.; An, L. H.; Burlingame, A. L.; Deng, Z. P.; Wang, Z. Y. Proteomics analysis reveals post-translational mechanisms for cold-induced metabolic changes in *Arabidopsis*. *Mol. Plant* **2011**, *4*, 361–374.
- (21) Deng, Z.; Zhang, X.; Tang, W.; Osés-Prieto, J. A.; Suzuki, N.; Gendron, J. M.; Chen, H.; Guan, S.; Chalkley, R. J.; Peterman, T. K.; Burlingame, A. L.; Wang, Z. Y. A proteomics study of brassinosteroid response in *Arabidopsis*. *Mol. Cell Proteomics* **2007**, *6*, 2058–2071.
- (22) Deng, Z.; Xu, S.; Chalkley, R. J.; Osés-Prieto, J. A.; Burlingame, A. L.; Wang, Z. Y.; Kutschera, U. Rapid auxin-mediated changes in the proteome of the epidermal cells in rye coleoptiles: implications for the initiation of growth. *Plant Biol. (Stuttg)* **2012**, *14*, 420–427.
- (23) Guan, S.; Price, J. C.; Prusiner, S. B.; Ghaemmaghami, S.; Burlingame, A. L. A data processing pipeline for mammalian proteome dynamics studies using stable isotope metabolic labeling. *Mol. Cell Proteomics* **2011**, *10*, M111.010728-1–M111.010728-8.
- (24) Chalkley, R. J.; Baker, P. R.; Huang, L.; Hansen, K. C.; Allen, N. P.; Rexach, M.; Burlingame, A. L. Comprehensive analysis of a multidimensional liquid chromatography mass spectrometry dataset acquired on a quadrupole selecting, quadrupole collision cell, time-of-flight mass spectrometer: II. New developments in Protein Prospector allow for reliable and comprehensive automatic analysis of large datasets. *Mol. Cell Proteomics* **2005**, *4*, 1194–1204.
- (25) Raggiaschi, R.; Lorenzetto, C.; Diodato, E.; Caricasole, A.; Gotta, S.; Terstappen, G. C. Detection of phosphorylation patterns in rat cortical neurons by combining phosphatase treatment and DIGE technology. *Proteomics* **2006**, *6*, 748–756.
- (26) Yamagata, A.; Kristensen, D. B.; Takeda, Y.; Miyamoto, Y.; Okada, K.; Inamatsu, M.; Yoshizato, K. Mapping of phosphorylated proteins on two-dimensional polyacrylamide gels using protein phosphatase. *Proteomics* **2002**, *2*, 1267–1276.
- (27) Kim, T. W.; Guan, S.; Sun, Y.; Deng, Z.; Tang, W.; Shang, J. X.; Burlingame, A. L.; Wang, Z. Y. Brassinosteroid signal transduction from cell-surface receptor kinases to nuclear transcription factors. *Nat. Cell Biol.* **2009**, *11*, 1254–1260.
- (28) Matsuoka, D.; Tokutomi, S. Blue light-regulated molecular switch of Ser/Thr kinase in phototropin. *Proc. Natl. Acad. Sci. U.S.A.* **2005**, *102*, 13337–13342.
- (29) Reymond, P.; Short, T. W.; Briggs, W. R.; Poff, K. L. Light-induced phosphorylation of a membrane protein plays an early role in signal transduction for phototropism in *Arabidopsis thaliana*. *Proc. Natl. Acad. Sci. U.S.A.* **1992**, *89*, 4718–4721.
- (30) Kodama, Y.; Suetsugu, N.; Kong, S. G.; Wada, M. Two interacting coiled-coil proteins, WEB1 and PMI2, maintain the chloroplast photorelocation movement velocity in *Arabidopsis*. *Proc. Natl. Acad. Sci. U.S.A.* **2010**, *107*, 19591–19596.
- (31) Inoue, S.; Matsushita, T.; Tomokiyo, Y.; Matsumoto, M.; Nakayama, K. I.; Kinoshita, T.; Shimazaki, K. Functional analyses of the activation loop of phototropin2 in *Arabidopsis*. *Plant Physiol.* **2011**, *156*, 117–128.
- (32) Saracco, S. A.; Hansson, M.; Scalf, M.; Walker, J. M.; Smith, L. M.; Vierstra, R. D. Tandem affinity purification and mass spectrometric analysis of ubiquitylated proteins in *Arabidopsis*. *Plant J.* **2009**, *59*, 344–358.
- (33) Peng, J.; Schwartz, D.; Elias, J. E.; Thoreen, C. C.; Cheng, D.; Marsischky, G.; Roelofs, J.; Finley, D.; Gygi, S. P. A proteomics approach to understanding protein ubiquitination. *Nat. Biotechnol.* **2003**, *21*, 921–926.
- (34) Gallagher, S.; Short, T. W.; Ray, P. M.; Pratt, L. H.; Briggs, W. R. Light-mediated changes in two proteins found associated with plasma membrane fractions from pea stem sections. *Proc. Natl. Acad. Sci. U.S.A.* **1988**, *85*, 8003–8007.
- (35) Kinoshita, T.; Emi, T.; Tominaga, M.; Sakamoto, K.; Shigenaga, A.; Doi, M.; Shimazaki, K. Blue-light- and phosphorylation-dependent binding of a 14-3-3 protein to phototropins in stomatal guard cells of broad bean. *Plant Physiol.* **2003**, *133*, 1453–1463.
- (36) Tseng, T. S.; Whippo, C.; Hangarter, R. P.; Briggs, W. R. The role of a 14-3-3 protein in stomatal opening mediated by PHOT2 in *Arabidopsis*. *Plant Cell* **2012**, *24*, 1114–1126.
- (37) Chen, Z. J.; Sun, L. J. Nonproteolytic functions of ubiquitin in cell signaling. *Mol. Cell* **2009**, *33*, 275–286.
- (38) Hershko, A.; Ciechanover, A. The ubiquitin system. *Annu. Rev. Biochem.* **1998**, *67*, 425–479.
- (39) Miranda, M.; Sorkin, A. Regulation of receptors and transporters by ubiquitination: New insights into surprisingly similar mechanisms. *Mol. Interventions* **2007**, *7*, 157–167.
- (40) Hoersch, D.; Bolourchian, F.; Otto, H.; Heyn, M. P.; Bogomolni, R. A. Dynamics of light-induced activation in the PAS domain proteins LOV2 and PYP probed by time-resolved tryptophan fluorescence. *Biochemistry* **2010**, *49*, 10811–10817.
- (41) Deng, Z.; Bu, S.; Wang, Z. Y. Quantitative analysis of protein phosphorylation using two-dimensional difference gel electrophoresis. *Methods Mol. Biol.* **2012**, *876*, 47–66.
- (42) Tang, W.; Deng, Z.; Osés-Prieto, J. A.; Suzuki, N.; Zhu, S.; Zhang, X.; Burlingame, A. L.; Wang, Z. Y. Proteomics studies of brassinosteroid signal transduction using prefractionation and two-dimensional DIGE. *Mol. Cell Proteomics* **2008**, *7*, 728–738.